

# Texture–Strength Properties of the Alumina–Montmorillonite Composite

V. A. Drozdov, V. P. Doronin, T. P. Sorokina, T. I. Gulyaeva, and V. K. Duplyakin

Boreskov Institute of Catalysis (Omsk Branch), Siberian Division,  
Russian Academy of Sciences, Omsk, 644053 Russia

Received September 6, 1999

**Abstract**—The texture characteristics and strength properties of the molded alumina–montmorillonite composite are studied. The mixture is obtained by mixing suspensions of activated clay and pseudoboehmite followed by drying (at 293 and 393 K) and calcination (at 873 K). It is a promising support for cracking and hydrotreating catalysts. The changes in the specific surface area; the volumes of micro-, meso-, macropore, and medium-size pores; and the strength of samples are studied by varying the montmorillonite concentration in the composite. The addition of 20–35 wt % clay largely results in a sharp reduction of the macropore region and, correspondingly, provides the alumina oxide average strength of the extrudates of  $\sim 10$ –12 MN/m<sup>2</sup>, which is sufficient for industrial supports. This excludes the stage of standard acidic peptization from the technological scheme of alumina production. The complex study of the porous structure of the composite by adsorption and mercury porosimetry combined with elements of percolation theory makes it possible to predict the texture–strength properties of derivative materials.

## INTRODUCTION

The alumina–montmorillonite composite is a promising support for catalysts of several oil refining processes (hydrotreating, hydrocracking, and catalytic cracking). Montmorillonite is a good binder because montmorillonite hydration results in the spontaneous decomposition of its particles to sizes smaller than 1  $\mu\text{m}$  and in considerable swelling of the system. The introduction of hydrated and activated montmorillonite into aluminum hydroxide enables the control of the porous structure and strength of the resulting composite.

General regularities of the porous structure formation of both alumina obtained from reprecipitated forms of aluminum hydroxide and montmorillonite obtained from its hydrated states are known [1–3].

In this work, we studied the formation of the texture of the alumina–montmorillonite composite with the aim of predicting the texture–strength properties of derivative supports.

## EXPERIMENTAL

### *Preparation of the Composite*

The following starting components of the support were used: nonpeptized pseudoboehmite aluminum hydroxide obtained by precipitation from aluminum sulfate and sodium aluminate and natural Na-montmorillonite activated by aluminum sulfate (a monomineral fraction from the Taganskoe deposit, Kazakhstan) with the chemical composition, wt %: SiO<sub>2</sub>, 66.0; Al<sub>2</sub>O<sub>3</sub>, 24.9; MgO, 3.5; Na<sub>2</sub>O, 1.8; Fe<sub>2</sub>O<sub>3</sub>, 1.7; and admixtures of calcium, titanium, and manganese oxides, 2.1 (total).

The starting clay was activated with aluminum sulfate by ion exchange to remove sodium cations, which are an undesirable admixture in the preparation and further application of these composites. The cation-exchange capacity was 90 mequiv/100 g clay, which corresponded to the exchange degree limiting for this montmorillonite sample. After activation, clay was multiply washed with doubly distilled water to remove sodium and sulfate ions.

Different compositions prepared by mixing suspensions of the starting components and containing 20 to 65 wt % montmorillonite (calculated per calcined montmorillonite–Al<sub>2</sub>O<sub>3</sub> composite) were extruded to granules (the size of extrudates after calcination was  $\sim 2.5$  mm). The molded samples of the two-phase aluminum hydroxide–montmorillonite system were dried in air for  $\sim 12$  h and then at 393 K for 3 h. After calcination in a muffle furnace at 873 K for 2 h, the final montmorillonite– $\gamma$ -Al<sub>2</sub>O<sub>3</sub> composites with different concentrations of clay were obtained. For comparison, the molded samples of the starting aluminum hydroxide and Al-montmorillonite were subjected to similar procedures of drying and thermal treatment.

### *Study of the Texture Characteristics and Strength*

The texture characteristics of the prepared supports were studied on a Sorptomatic-1900 adsorption instrument by nitrogen adsorption–desorption isotherms at 77.4 K and on a model 2000 mercury porosimeter.

Adsorption measurements were performed using granules and the 0.40–0.25-mm fraction of samples. Before experiments, calcined samples were treated for

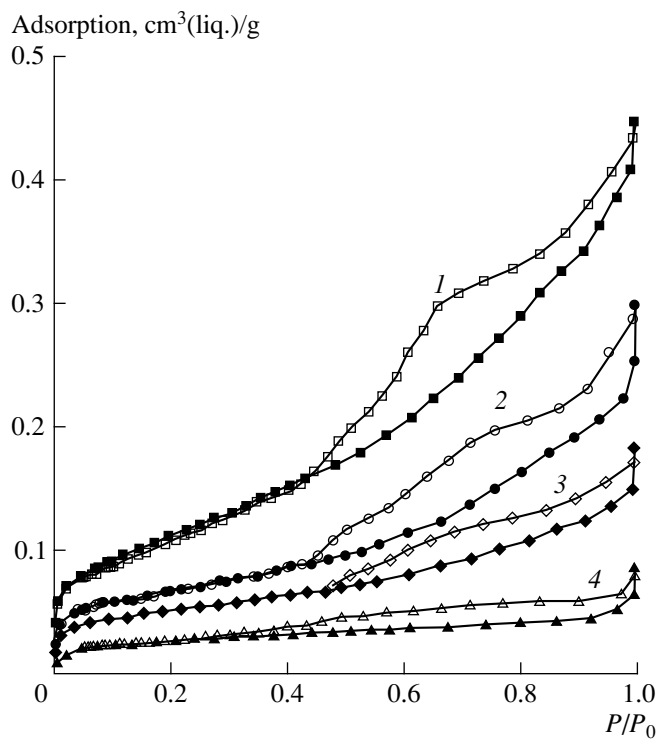


**Fig. 1.** Nitrogen adsorption–desorption isotherms at 77.4 K on the samples: (1)  $\text{Al}_2\text{O}_3$ ; (2) 35 wt % montmorillonite; (3) 65 wt % montmorillonite; and (4) montmorillonite.

10 h at 623 K in a vacuum under a residual pressure of at most  $10^{-1}$  Pa.

The BET specific surface area ( $S_{\text{BET}}$ ) was calculated from the adsorption isotherm in the interval of relative equilibrium pressures of nitrogen vapor  $P/P_0 = 0.05–0.33$ . In the calculation of the specific surface area, we assumed that the area required for the molecular adsorption of nitrogen in a filled monolayer is  $0.162 \text{ nm}^2$ . The adsorption pore volume ( $V_{\text{ads}}$ ) was found from the nitrogen adsorption at  $P/P_0 = 0.996$ . The molar volume of the liquid adsorbate at the experimental temperature was taken to be equal to  $34.68 \times 10^{-6} \text{ m}^3/\text{mol}$ . The size distribution of mesopores was calculated by the Dollimore–Heal method [4]. Comparative analysis [5, 6] of adsorption isotherms was used for the determination of the micropore volume ( $V_{\text{micro}}$ ) and the specific mesopore surface area ( $S_{\text{meso}}$ ). To consider changes in the porous structure in the macropore region ( $V_{\text{macro}}$ ,  $S_{\text{macro}}$ ) and obtain data on the total pore volume ( $V_{\Sigma}$ ) and porosity ( $\epsilon$ ) of the samples under study, we used mercury porosimetry together with adsorption studies. The following surface tension of mercury and wetting angle were assumed:  $\sigma = 480 \text{ MN/m}$  and  $\theta = 141.3^\circ$ . The cylindrical model of pores [5] was used in both adsorption and mercury porosimetry calculations. In the study of the porous structure of the composites, we used the IUPAC classification of pores over sizes [7, 8].

The mechanical strength of samples was determined using an MP-9S instrument by the method of squashing along generatrix. The obtained results were statistically processed by averaging over 25 measurements.

The samples were subjected to X-ray phase analysis on a DRON-3 diffractometer (Ni filter,  $\text{CuK}_\alpha$  radiation,  $\lambda = 0.154 \text{ nm}$ ). The interplanar distance  $d_{001}$  for the first basal reflection in the initial and activated montmorillonites was determined from the angular position of the diffraction peak in the region  $2\theta = 5^\circ–7^\circ$ .

## RESULTS AND DISCUSSION

### Structural Parameters of Starting Substances

According to the XRD data, after the ion exchange of starting Na-montmorillonite for the activated Al-form, an increase in the interplanar distance is not observed. The value of the first basal reflection for the samples of both Al- and Na-montmorillonites is  $d_{001} = 1.28 \text{ nm}$ . The specific surface area and effective micropore volume of the Al-montmorillonite samples dried at 393 K are  $49 \text{ m}^2/\text{g}$  and  $0.02 \text{ cm}^3/\text{g}$ , respectively. The activated clay samples also have a macropore region with a volume of  $\sim 0.025 \text{ cm}^3/\text{g}$  and a specific surface area of  $\sim 0.6 \text{ m}^2/\text{g}$ .

According to the XRD data, precipitated aluminum hydroxide has a pseudoboehmite structure. The specific surface area is  $\sim 350 \text{ m}^2/\text{g}$ , and the volumes of meso- and micropores are  $0.30$  and  $0.14 \text{ cm}^3/\text{g}$ , respectively. We also observed a small macropore volume of  $\sim 0.10–0.12 \text{ cm}^3/\text{g}$  stipulated by large (100–1000 nm) aggregates formed from primary needle-like pseudoboehmite particles.

### Adsorption Study of the Texture of Composites

The nitrogen adsorption–desorption isotherms at 77.4 K for particular samples are presented in Fig. 1. Isotherms for the samples with a clay concentration of up to 50 wt % largely repeat the shape of the isotherm on alumina. These are the type IV isotherms containing a complex-shape hysteresis loop, intermediate between H2 and H3 according to the IUPAC classification. These isotherms reflect the presence of mesopores with different sizes, shapes, and cohesion [7, 8]. The amount of adsorbed substance decreases with an increase in the clay concentration in the composite. For the samples with a clay concentration of 65 wt % and higher, the isotherms acquire a shape closer to that of the adsorption isotherm for activated montmorillonite, which is classified as a type I isotherm with the hysteresis loop H4, which reflects microporosity [5, 8].

Table 1 presents the main texture characteristics of the studied supports obtained from the analysis of adsorption isotherms.

The data in Table 1 show that the  $\gamma\text{-Al}_2\text{O}_3$  component with a high intrinsic porosity plays the determining role in the formation of the micro- and mesoporous spaces of the composites. However, note that the intro-

duction of even a small amount of clay substantially changes the characteristics of the porous structure of the samples.

Let us consider in more detail a change in the texture characteristics of the studied samples with a variation in their composition. The specific surface areas  $S_{\text{BET}}$  and  $S_{\text{meso}}$  of the samples change virtually in the same direction when the composition is changed. These values exhibit a regular decrease with an increase in the montmorillonite concentration. However, at small clay concentrations (to 35 wt %), a decrease in the surface area is sharper than that in the samples containing  $\geq 50$  wt % clay; that is, a small inflection point is observed on the plot of specific surface area vs. composition at a montmorillonite concentration of 35–50 wt %.

The data in Table 1 show that a change in the micropore volume in the materials containing more than 20 wt % clay is linear and decreases to  $\sim 0.02 \text{ cm}^3/\text{g}$ , which is characteristic of pure clay, with an increase in the montmorillonite concentration. We do not expect for this method of composite preparation by mixing two suspensions followed by thermal treatment that the micropore volume changes in a way other than according to the additivity law (of the mechanical mixture). A change in the mesopore volume (calculated as  $V_{\text{meso}} = V_{\text{ads}} - V_{\text{micro}}$ ) can also be generally approximated by a linear function, but for the compositions with 35 and 50 wt % a plateau appears with an almost unchanged mesopore volume  $V_{\text{meso}}$  of  $\sim 0.2 \text{ cm}^3/\text{g}$ . Note that an approximately unchanged specific surface area is also observed for these samples (Table 1).

Table 1 also contains the effective mean sizes of mesopores obtained from nitrogen adsorption–desorption isotherms. In addition, Figs. 2 and 3 present the functions of the mesopore volume distribution over effective sizes for various samples of the system. In general, they demonstrate the character of a change in the mesoporosity of the composite when its composition is varied. Of course, it should be taken into account that the calculated data of the mesopore distributions over both adsorption and desorption isotherm branches

are approximate because of the complicated shape of the hysteresis loop of experimental isotherms (Fig. 1) [8, 9]. Note also that, according to the published data [10], the use of commonly accepted methods for the calculation of the size distribution of mesopores from the desorption branch of isotherms for layered materials, in particular, clays, results in the appearance of a false maximum (artifact) in the region of pores with a diameter of  $\sim 3.9 \text{ nm}$ . However, this problem requires a special study and we do not consider it here. When the montmorillonite concentration in the composite increases, the values on the distribution of the mesopore volume in the region of the most pronounced effective sizes (3–10 nm) decrease substantially. This is accompanied by some redistribution of mesopores, but without a characteristic change in their position relatively to the scale of pore diameters. For example, the average desorption size of mesopores ( $D_{\text{des}}$ ) in the samples changes by at most 7–10% when the clay concentration varies from 0 to 65 wt % and almost coincides with the effective average diameter of the pores obtained from the expression  $D_{\text{av}} = 4V_{\text{ads}}/S_{\text{BET}}$  (Table 1). A change in the adsorption size of the mesopores ( $D_{\text{ads}}$ ) in the samples with different concentrations of montmorillonite is somewhat greater and equals  $\sim 10$ –13%. The results show that the mesopore sizes in the composite calculated from isotherms are largely determined by the average size of mesopores of alumina, which is the most porous component.

Thus, a monotonic decrease in the mesoporosity with an increase in the montmorillonite concentration in the composite (except for the narrow region of  $42 \pm 8$  wt % clay) accompanied by an insignificant size redistribution reflects, in fact, the variant of the additive substitution of one higher-mesoporosity component (alumina) by another (montmorillonite) with a lower porosity and a close effective size of the mesopores. Virtually unchanged characteristics of mesopores for the compositions with 35–50 wt % clay are most likely related to additional mesoporosity near the interface of the particles of components that have different shapes

**Table 1.** Main texture characteristics of the alumina–montmorillonite composite according to adsorption data

Clay concentration, wt %	$S_{\text{BET}}$ , $\text{m}^2/\text{g}$	$S_{\text{meso}}$ , $\text{m}^2/\text{g}$	$V_{\text{micro}}$ , $\text{cm}^3/\text{g}$	$V_{\text{ads}}$ , $\text{cm}^3/\text{g}$	$D^*$ , nm	$D_{\text{des}}, D_{\text{ads}}$ , nm
0	264	261	0.060	0.445	6.7	6.3 8.9
20	195	164	0.073	0.353	7.2	7.5 9.6
35	150	114	0.060	0.251	6.7	7.0 10.3
50	139	105	0.050	0.242	7.0	6.5 11.2
65	113	81	0.041	0.183	6.5	6.7 9.7
100	59	51	0.017	0.085	5.8	4.5 4.9

\*  $D$  is the average pore diameter calculated by the formula  $D = 4V_{\text{ads}}/S_{\text{BET}}$ ;  $D_{\text{des}}$  and  $D_{\text{ads}}$  are the average pore diameters calculated from the desorption and adsorption branches of isotherms.

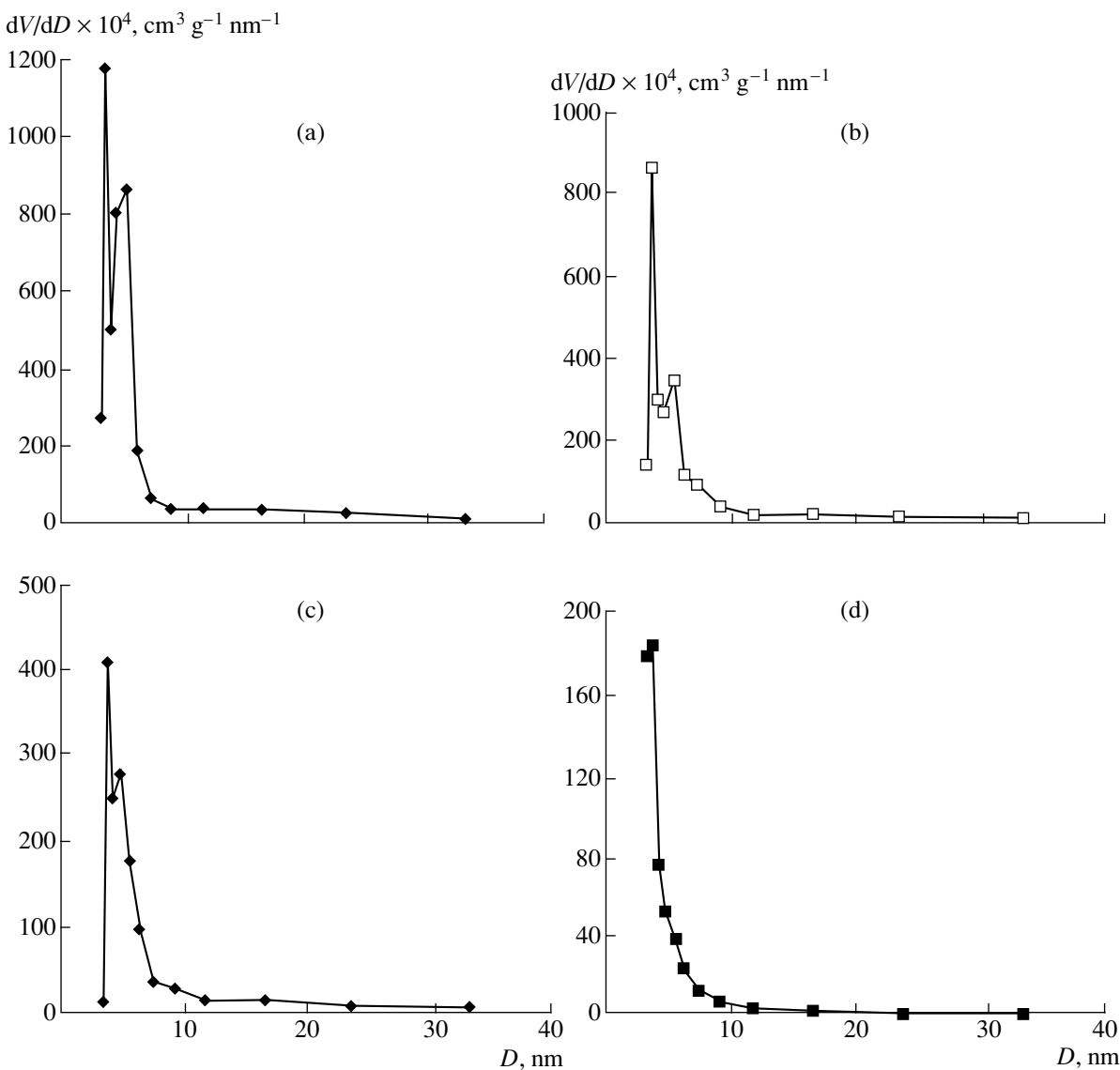


**Fig. 2.** Distributions of the mesopore volume in the samples calculated from the desorption branches of isotherms ( $N_2$ , 77.4 K): (a) alumina; (b) 50 wt % montmorillonite; (c) 65 wt % montmorillonite; and (d) montmorillonite.

(thin plates for montmorillonite, agglomerates of needle-like piles for alumina) when their concentrations in the composite are commensurable.

#### *Study of the Texture of the Composites by Mercury Porosimetry*

The results of the study of the texture characteristics of the supports by mercury porosimetry are presented in Table 2.

Figure 4 presents changes in the specific pore volume of the samples when their compositions are varied. The data were obtained from the porosimetric measurements of the mercury impression curves, including changes in the specific volume and specific surface area calculated only for the macropore region. Let us con-

sider a change in the main texture characteristics of the macropores in calcined pure alumina and the composite containing some amount of clay. For the support sample containing only 20 wt % montmorillonite, the macropore volume is ~4.7 times smaller than for pure alumina oxide and the total pore volume is approximately three times smaller as determined by this method. The specific surface area of the macropores in the composite is two times smaller, and the average macropore size decreased from 339 to 146 nm (Table 2).

Thus, the introduction of even a small amount of montmorillonite into the starting aluminum hydroxide substantially affects the formation of macroporosity in a composite. As the clay concentration increases from 20 to 70 wt %, a further decrease (by about two times) in the specific volume of the pores is observed first of

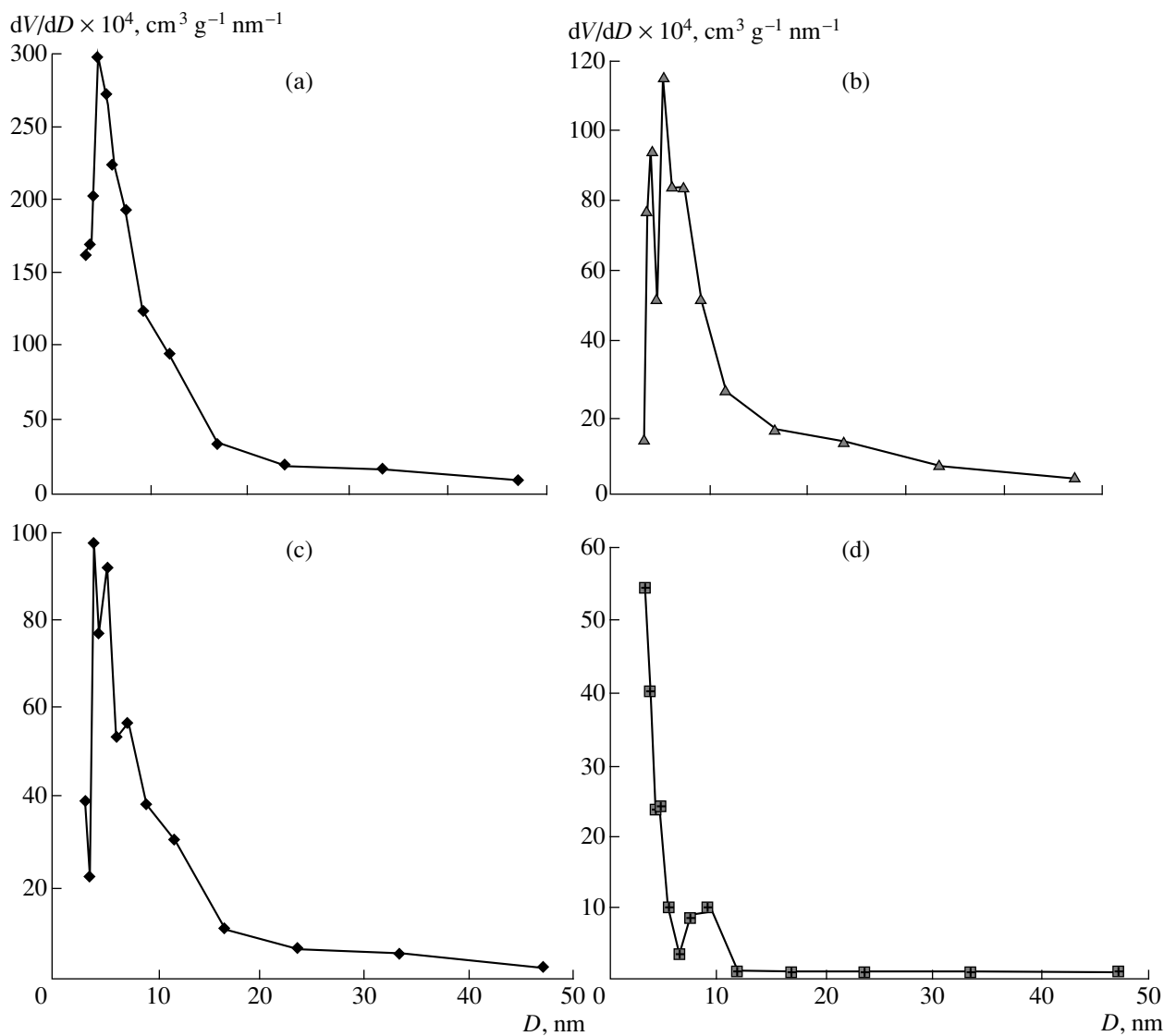


**Fig. 3.** Distributions of the mesopore volume in the samples calculated from the adsorption branches of the isotherms ( $\text{N}_2$ , 77.4 K): (a) alumina; (b) 50 wt % montmorillonite; (c) 65 wt % montmorillonite; and (d) montmorillonite.

all due to a substantial (~16-fold) decrease in the macropore volume. The specific surface area of the macropores decreases almost by a factor of 10 and becomes as small as  $\sim 0.3$ – $0.5 \text{ m}^2/\text{g}$ . It is important that a further decrease in the average size of macropores is observed from 150 to 75–90 nm. Some further increase in the macroporosity for the compositions with the 80–100% clay concentration is related to the influence of intrinsic macropores of montmorillonite.

A decrease in the main parameters of macropores can be attributed to either the effects of filling the macropores of one component with the particles of another or structural rearrangement of the elements that form the macroporous space during the physicochemical interaction of the components. To examine possible reasons for the substantial change in the macroporous area of the composites, let us consider a change in the

porosity ( $\epsilon$ ) of the systems, which is a more general structural parameter than the specific pore volume ( $V$ ) because the latter depends on the true density ( $\rho$ ) of the samples that changes with a change in the clay concentration.

#### Change in the Porosity of the Composites

The porosity of composites was determined from the adsorption and mercury porosimetry data using the equation

$$\epsilon = V_{\Sigma} \rho_{\text{av}} / (1 + V_{\Sigma} \rho_{\text{av}}) = V_{\Sigma} [\rho_{\text{mont}} X + \rho_{\text{Al}_2\text{O}_3} (1 - X)] / (1 + V_{\Sigma} [\rho_{\text{mont}} X + \rho_{\text{Al}_2\text{O}_3} (1 - X)]), \quad (1)$$

where  $V_{\Sigma} = V_{\text{micro}} + V_{\text{meso}} + V_{\text{macro}}$  is the total specific pore volume;  $X$  is the molar fraction of clay, and  $(1 - X)$

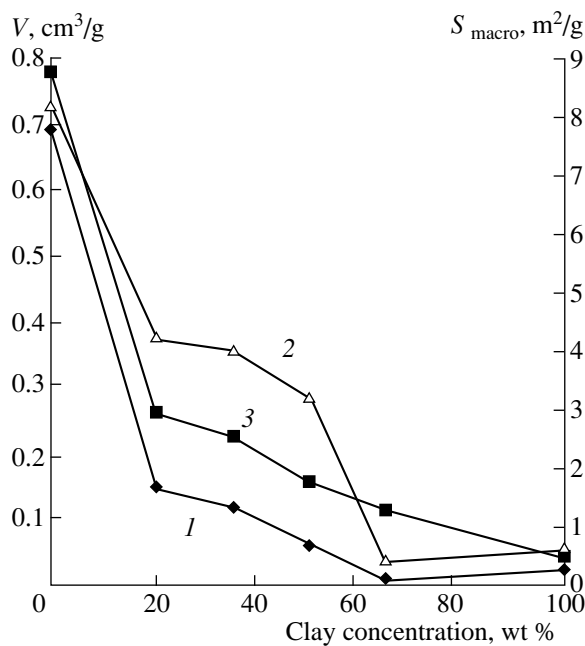


**Fig. 4.** Changes in the (1) specific volume and (2) specific surface area of macropores, and (3) total pore volume with the variation of the clay concentration in the alumina–montmorillonite composite by the mercury porosimetry data.

is the weight fraction of alumina; and  $\rho_{\text{mont}}$  and  $\rho_{\text{Al}_2\text{O}_3}$  are the true densities of the components equal to 2.50 and 3.54 g/cm<sup>3</sup>, respectively. In addition, we obtained the simplest estimates of a change in the porosity in the model binary dispersed alumina–montmorillonite system (a mixture of two narrow fractions of particles that differ in sizes by a factor of ~10) provided fine particles are arranged in cavities between large particles and do not affect the packing of the latter. For the calculation of the porosity change as functions of the composition

**Table 2.** Specific porosity, volume, average macropore diameter, and total specific volume of pores in the samples under study

Clay concentration, wt %	$S_{\text{macro}}$ , m <sup>2</sup> /g	$V_{\text{macro}}$ , cm <sup>3</sup> /g	$D_{\text{macro}}$ , nm	$*V_{\Sigma}$ , cm <sup>3</sup> /g
0	8.2	0.690	339	$0.99 \pm 0.05$
20	4.2	0.146	146	$0.41 \pm 0.01$
35	4.0	0.117	111	$0.28 \pm 0.02$
50	3.2	0.060	74	$0.24 \pm 0.02$
65	0.4	0.009	90	$0.17 \pm 0.01$
100	0.6	0.023	153	$0.12 \pm 0.02$

\*  $V_{\Sigma} = V_{\text{micro}} + V_{\text{meso}} + V_{\text{macro}}$ ; this value was calculated from the data of mercury and adsorption porosimetry.

and determination of the critical concentration of the chosen fraction, we used the equations proposed in [11]

$$x < x_{\text{cr}} \quad \epsilon = \epsilon_{01} [1 - (x/1-x) \times (\rho_1/\rho_2)(1 - \epsilon_{01}/\epsilon_{01})], \quad (2)$$

$$x_{\text{cr}} = 1/[1 + (\rho_1/\rho_2)(1 - \epsilon_{01})/(1 - \epsilon_{02})(1/\epsilon_{01})], \quad (3)$$

$$\text{for } x > x_{\text{cr}} \quad \epsilon = \epsilon_{02} [1 + (1-x/x) \times (\rho_2/\rho_1)(1 - \epsilon_{02})], \quad (4)$$

where  $x$  is the weight fraction of small particles;  $x_{\text{cr}}$  is the concentration of the fine fraction when the space between large particles is entirely filled;  $\rho_1$  and  $\rho_2$  are the true densities for the large and fine particles, respectively; and  $\epsilon_{01}$  is the porosity characteristic of the packing of the large particles at  $x = 0$ , and  $\epsilon_{02}$  is the intrinsic porosity of the fine particles.

Figure 5 presents changes in the porosity of the real composite (experimental) and the model system (calculated) as a function of their compositions. The difference between the calculated critical concentrations of the fine fraction for different types (clay or alumina) is related to different true densities and, to a larger degree, on the porosities of these components in the composite.

First, the character of a change in the experimental porosities of the studied compositions differs strongly from that of the calculated values for the model. The shape of the plot excludes the appearance of a minimum, reflecting the presence of the critical concentration of the fine fraction, which must always be present according to the model assumption. Therefore, we are sure that a decrease in the porosity with an increase in the clay concentration in the samples, which was found to be primarily due to a decrease in the macropore volume, is not determined by the simple model of the formation of the binary dispersed system in which smaller particles are arranged in gaps (macropores) between large particles.

We believe that a decrease in the porosity with an increase in the montmorillonite concentration in the samples due to the disappearance of the macroporous area is determined by a strong peptizing effect of activated clay on the aggregates of aluminum hydroxide under the conditions of composite preparation. In fact, activated clay, being a weak H<sup>+</sup> acid, can most likely play the role of a peptizing agent for aluminum hydroxide by the known acidic mechanism of peptization with organic or mineral acids, that is, through the formation of surface hydroxy and oxy salts of aluminum [1]. However, the surface electrostatic interactions most likely play a more important role in hydroxide peptization with clay. Crystals of clay minerals are known [3] to gain a negative charge during heterovalent isomorphism. This charge is compensated by exchange cations that not only enter the interlayer space of the structure, although they are also arranged both on the external facets and even at a some distance from the surface to form the so-called diffuse layer of a clay micelle and

water molecules. By contrast, the particles of precipitated aluminum hydroxide in acidic media usually have a positive surface charge compensated by either the hydroxy ion or doped anions. As a result, during the preparation of the composites from the starting clay and hydroxide suspensions, strong electrostatic interactions can occur between the ion-hydrated surface layers of clay and aggregates of aluminum hydroxide. These interactions can destroy the latter. Thus, we assume that first large, but unstable, particles/aggregates of aluminum hydroxide are structurally rearranged under the effect of montmorillonite in the system under study. As a result, further thermal treatments of the system form the lower-porosity composite alumina-montmorillonite with a substantially lower macroporosity than unmodified and nonpeptized alumina. Of course, this effect should substantially affect the strength parameters of the formed materials.

#### Strength of the Composite under Study

Table 3 contains the maximum, minimum, and average strengths of the alumina samples with different compositions calcined in air at 873 K for 2 h.

As can be seen, the addition of even 20 wt % (up to 30 vol %) montmorillonite leads to an increase in the strength of the extruded samples by three- to four times. The average strengths of the composites with 20–35 wt % (up to 43 vol %) of clay are close to those characteristic of the strength of the alumina samples prepared from aluminum hydroxide peptized with acid [1].

We may assume that processes associated with a change in the secondary structure of alumina, such as deaggregation of large particles that decreases the macroporosity of alumina and the total porosity of the composite, plays a critical role in an increase in the strength of these composites. Indeed, according to data from mercury porosimetry (Table 2), in the samples containing from 20 to 35 wt % montmorillonite, the macropore volume decreases~4–6 times compared with the starting alumina, whose macropore volume is  $0.69 \text{ cm}^3/\text{g}$ , and reaches only about  $0.12\text{--}0.15 \text{ cm}^3/\text{g}$ . Currently, it is well known that [12] large pores not merely decrease the number of contacts but also are the sources of strains (cracks) leading to a sharp decrease in the strength. A further increase in the clay concentration to 50 wt % (~60 vol %) is not accompanied by an increase in the strengths of the samples, although the macropore volume continues to decrease and equals  $\sim 0.06 \text{ cm}^3/\text{g}$ . Evidently, these compositions exhibit neither a pronounced increase in the strength of individual contacts between the characteristic texture fragments (particles of alumina and clay) nor a substantial change in the distribution over their number, which could change the strength. In the interval of the clay concentration from 50 to 65 wt % (up to 70 vol %), the strength of the composite samples again increases (by a factor of ~1.3–1.4). This increase can be associated with the formation of new, stronger individual contacts between

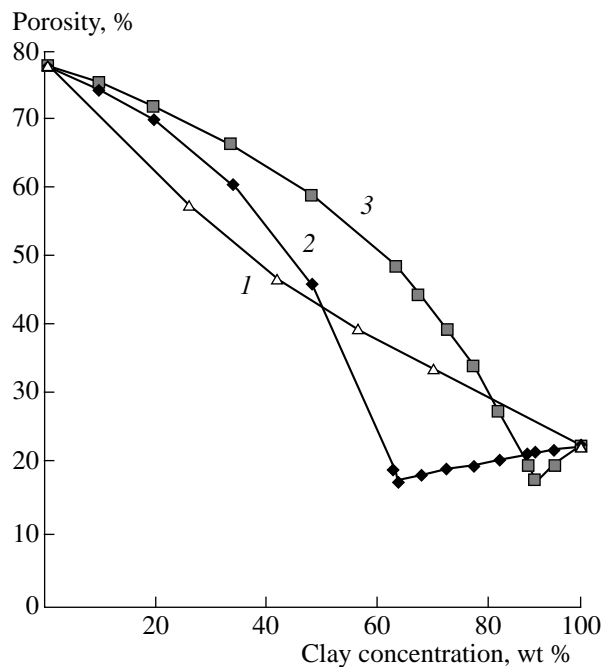


**Fig. 5.** Changes in the porosity of the system under study at different concentrations of montmorillonite: (1) experiment; (2 and 3) calculation ((2) fine fraction—clay particles; (3) fine fraction—alumina particles).

the characteristic texture elements (primary particles) of montmorillonite and, additionally, with the almost complete disappearance of the macroporous area of alumina because the macropore volume in the samples does not exceed  $0.01 \text{ cm}^3/\text{g}$ . Perhaps, these objects have a single skeleton structure of the support primarily due to the introduced montmorillonite. At a higher concentration of clay (>65 wt %), we observed an additional increase in the maximal and average strengths (by ~1.5 and 1.3 times, respectively), whereas the minimal strength remains almost unchanged (Table 3). This fact can indicate further strengthening of the structure of the solid clay skeleton when its concentration approaches the limit (100 wt %).

This discussion of changes in the strength of the alumina-montmorillonite composite with the variation of its composition and texture is phenomenological because rigorous quantitative physicochemical theory for the strength of dispersed materials is far from being settled, especially for multicomponent and multiphase porous systems [12]. Therefore, we attempted to explain the character of changes in the strength of this composite with the variation of the composition and texture based on the simplest model concepts of percolation theory within the framework of the problem of nodes [13–15]. This attempt was made to understand whether this change is general and whether the texture-strength properties of similar composites can be predicted.

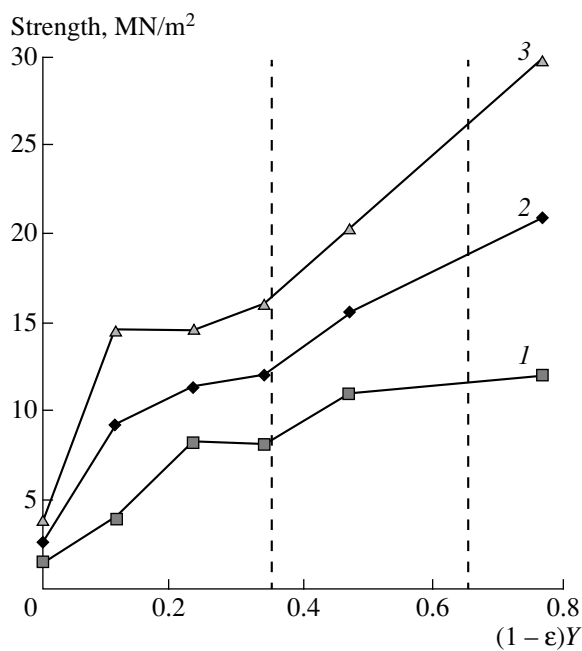


**Fig. 6.** Changes in the mechanical strength of the samples at different volume concentrations of montmorillonite in the solid skeleton of the composite: (1) minimum; (2) average; and (3) maximum.

In the framework of percolation theory for the problem of nodes, there must exist a threshold of a change in the strength of the infinite system consisting of two solid porous components with the variation of their volume concentration (e.g., the volume concentration of montmorillonite  $Y$ ) and some certain invariant independent of the specific geometry of the lattice. We took  $(1 - \varepsilon)Y$  corresponding to the volume fraction of the montmorillonite component in the composition of the solid skeleton of the composite as an invariant of similar composites.

For further consideration, we designate alumina as phase A and montmorillonite as phase M. Changes in the strength of the studied samples at different volume con-

centrations of montmorillonite in the solid skeleton of the composite are presented in Fig. 6. According to percolation theory, if the volume fraction of phase M in the composition of the solid lattice is equal to  $(1 - \varepsilon)Y \leq 0.16$ , all nodes of phase M are separated, and the permeability (in our case, the strength) of the lattice is only determined by phase A. Indeed, the experiment shows that, for these compositions, a change in the strength is stipulated by the structural rearrangement of alumina accompanied by a decrease in the porosity. For the volume fraction of phase M  $0.16 < (1 - \varepsilon)Y < 0.35$ , isolated clusters of phase M and the formed “bound” cluster of the same phase coexist with phase A. The curves of a change in the strength for these clay concentrations (Fig. 6) most likely show its insignificant increase only due to the partial strengthening of the composite by the formed three-dimensional cluster of the introduced clay. At the concentration  $0.65 > (1 - \varepsilon)Y > 0.35$ , almost all of phase M becomes mutually bound; that is, it enters in the “infinite permeable cluster.” The strength must increase and be determined by the stability of the structures of the coexisting phases, A and M. In fact, it is seen in Fig. 6 that the plots of the strength have an inflection point at the volume fraction of the clay  $(1 - \varepsilon)Y = 0.35$  in the solid skeleton, and then the strength increases substantially with an increase in the montmorillonite concentration. At a higher clay concentration when  $(1 - \varepsilon)Y > 0.65$ , the strength of the samples should to a great extent be determined by the single solid clay skeleton for which the intrinsic mechanical strength is much higher (by almost an order of magnitude) than the strength of the particles of the partially retained phase of alumina.

Thus, percolation theory approximately describes the observed threshold (critical) changes in the strength properties of the two-phase alumina–montmorillonite system. It is noteworthy that simple concepts of percolation theory applied to the analysis of the strength of the studied solid porous composites is not fully correct because the estimation of critical phenomena requires considering the binding of large blocks without details of the fine-scale structure, that is, ignoring such an

**Table 3.** Influence of the clay concentration on the strength properties of the alumina–montmorillonite composite samples

Clay concentration		Maximum strength, MN/m <sup>2</sup>	Minimum strength, MN/m <sup>2</sup>	Average strength, MN/m <sup>2</sup>
wt %	Y*, vol %			
0	0	3.8	1.4	2.6
20	27	14.5	3.9	9.2
35	43	14.5	8.1	11.3
50	59	16.0	8.0	12.0
65	72	20.2	11.0	15.6
100	100	29.8	12.0	20.9

\* The calculation from the weight concentration (or weight fraction  $X$ ) of clay to the volume percentage ( $Y$ , vol %) was performed by the formula  $Y = X\rho_{\text{Al}_2\text{O}_3}/[X\rho_{\text{Al}_2\text{O}_3} + (1 - X)\rho_{\text{clay}}]$ .

important parameter of the solid skeleton as the structure and strength of the single contact of particles.

## CONCLUSION

The preparation of the two-component composite alumina–montmorillonite with the controlled parameters of the porous structure and strength properties is an important and necessary stage in the development of the technology for the manufacture of modern, highly efficient, and stable catalysts for cracking. Our results show that the interaction of activated montmorillonite with the initial aluminum hydroxide destroys the aggregates of the hydroxide. Therefore, the macroporosity of the calcined system substantially decreases and the mechanical strength of the composite increases. The introduction of montmorillonite (up to 20–35 wt %) into the composite results in the average strength of extrudates of  $\sim 10$ –12 MN/m<sup>2</sup>, which is sufficient for industrial supports. The stage of standard acidic peptization can thus be excluded from the technological scheme of the production of alumina, which is used as an adsorbent and support for cracking and hydrotreating.

This detailed study of the texture of the composites and its changes with the variation of the composition using the elements of percolation theory makes it possible to predict of the texture–strength properties of the related materials.

## ACKNOWLEDGMENTS

We thank V.Yu. Davydova for measurements of the strength properties of the objects under study.

## REFERENCES

1. Dzis'ko, V.A., *Osnovy metodov prigotovleniya katalizatorov* (Foundations of Catalyst Preparation), Novosibirsk: Nauka, 1983, p. 260.
2. Tarasevich, Yu.I. and Ovcharenko, F.D., *Adsorbsiya na glinistykh materialakh* (Adsorption on Clay Materials), Kiev: Naukova Dumka, 1975, p. 352.
3. Osipov, V.I., *Priroda prochnostnykh i deformatsionnykh svoistv glinistykh porod* (The Nature of Strength and Deformation Properties of Clays), Moscow: Moscow State University, 1979.
4. Dollimore, D. and Heal, G.R., *J. Colloid Interface Sci.*, 1973, vol. 33, no. 1, p. 233.
5. Gregg, S.J. and Sing, K.S.W., *Adsorption, Surface Area, and Porosity*, London: Academic, 1982.
6. Karnaughov, A.P., Fenelonov, V.B., and Gavrilov, V.Yu., *Pure Appl. Chem.*, 1989, vol. 61, no. 11, p. 1913.
7. Sing, K.S.W., Everett, D.H., Haul, R.A.W., et al., *Pure Appl. Chem.*, 1985, vol. 57, no. 4, p. 603.
8. Sing, K.S.W. and Rouquerol, J., *Handbook of Heterogeneous Catalysis*, Ertl, G., Knozinger, H., and Weitkamp, J., Eds., Weinheim: Wiley-VCH, 1997, vol. 2, p. 427.
9. Sing, K.S.W., *Colloids Surf.*, 1989, vol. 38, p. 113.
10. Carrado, K.A., Marshall, C.L., Brenner, J.R., and Song, K., *Microporous Mesoporous Mater.*, 1998, vol. 20, p. 17.
11. Fenelonov, V.B., *Nauchnye osnovy prigotovleniya katalizatorov* (Scientific Foundations of Catalyst Preparation), Novosibirsk: Institute of Catalysis, 1984, p. 130.
12. Shchukin, E.D., *Kinet. Katal.*, 1965, vol. 6, no. 4, p. 641.
13. Shante, V.K.S. and Kirkpatrick, S., *Adv. Phys.*, 1971, vol. 120, p. 325.
14. Efros, A.L., *Fizika i geometriya besporyadka* (Physics and Geometry of Disorder), Moscow: Nauka, 1982, p. 175.
15. Mason, G., *Stud. Surf. Sci. Catal.*, 1988, vol. 39, p. 323.